Indian J. Phys. **82 (4)** 435-445 (2008)

IJP

Injection/suction effect on an oscillatory hydromagnetic flow in a rotating horizontal porous channel

K D Singh* and Alphonsa Mathew

Department of Mathematics (ICDEOL), Himachal Pradesh University, Shimla 171 005, Himachal Pradesh India

E-mail kdsinghshimla@gmail.com

Received 11 July 2007, accepted 15 January 2008

Abstract : This paper studies the effects of injection/suction on an oscillatory flow of a viscous incompressible fluid in a porous channel The porous channel with constant injection/suction rotates about an axis perpendicular to the plates of the channel A magnetic field of uniform strength is also applied perpendicular to the plates The upper plate is allowed to oscillate in its own plane with the velocity $U^*(t^*)$ whereas the lower plate is at rest The effects of coriolis force and the magnetic field on the flow are studied

Keywords : Oscillatory, rotating, porous channel, injection/suction, hydromagnetic

PACS Nos. : 47.35 Tv, 47.65 -d

1. Introduction

Magnetofluid-dynamics (MFD) or Magnetohydrodynamics (MHD) has gained considerable importance because of its wide ranging applications in physics and engineering. In astrophysics and geophysics it is applied to study the stellar and solar structures, interplanetary, and inter stellar matter, solar storms and flares, radio propagation through the ionosphere *etc.* In engineering it finds its application in MHD generators, Ion propulsion, MHD bearings, MHD pumps, MHD boundary layer control of reentry vehicles *etc.* MHD has attracted the attention of large number of scholars due to its diverse applications. Attia and Kotb [1] studied the MHD flow between two parallel porous plates. Yen and Chang [2] analyzed the effects of wall electrical conductances on the magnetohydrodynamic couette flow. A magnetohydrodynamic flow in a duct has also been studied by Chang and Lundgren [3]. In the recent years a number of studies have appeared in the literature on the fluid phenomena on earth involving rotation to a greater or lesser extent *viz.* Vidyanidhu and Nigam [4], Gupta [5], Jana

*Corresponding Author

and Datta [6]. Injection/suction effects have also been studied extensively for horizontal porous plate in rotating frame of references by Gupta [7], Mazumder [8], Mazumder *et al* [9], Soundalgekar and Pop [10] for different physical situations. The fluid flows in rotating channels have been studied by a number of scholars *viz.* Mazumder [11] Ganapathy [12], Singh [13]. Singh *et al* [14] also obtained an exact periodic solution of oscillatory Ekman boundary layer flow through a porous medium bounded by two horizontal flat plates. In this paper it is proposed to study the injection/suction effects on a hydromagnetic oscillatory flow in a horizontal porous channel in a rotating system.

2. Mathematical analysis

We consider an oscillatory flow of a viscous incompressible and electrically conducting fluid between two insulating infinite parallel porous plates at a distance d apart A constant injection velocity, w_0, is applied at the lower stationary plate and the same constant suction velocity, w_0, is applied at the upper plate which is oscillating in its own plane with a velocity $U^*(t^*)$ about a non-zero constant mean velocity U_0. Choose the origin on the lower plate lying in x^*–y^* plane and x^*-axis parallel to the direction of motion of the upper plate. The z^*-axis taken perpendicular to the planes of the plates, is the axis of rotation about which the entire system is rotating with a constant angular velocity Ω^*. A transverse magnetic field of uniform strength B_0 is also applied along the axis of rotation. The value of this uniform magnetic field is assumed to be unaltered by making the necessary assumptions that guarantee the neglection of the induced electric and magnetic fields. Hall effect, electrical and polarization effects are also neglected. Since the plates are infinite in extent, all the physical quantities except the pressure, depend only on z^* and t^*. Denoting the velocity components u^*, v^* w^* in the x^* y^*, z^* directions, respectively, the flow in the rotating system is governed by the following equations :

$$w_z^* = 0, \tag{1}$$

$$u_t^* + w^* u_z^* = p_x^*/\rho + \upsilon u_{zz}^* + 2\Omega^* v^* - \sigma B_0^2 u^*/\rho \tag{2}$$

$$v_t^* + w^* v_z^* = -p_y^*/\rho + \upsilon v_{zz}^* - 2\Omega^* u^* - \sigma B_0^2 v^*/\rho \tag{3}$$

where υ is the Kinematic viscosity, t is the time, ρ is the density and p^* is the modified pressure, σ is the electric conductivity. The boundary conditions for the problem are

$$\left.\begin{aligned} u^* = v^* = 0, \quad w^* = w_0, \quad \text{at} \quad z^* = 0, \\ u^* = U^*(t^*) = U_0\left(1 + \varepsilon \cos \omega^* t^*\right) \end{aligned}\right\} \tag{4}$$

$$\nu^* = 0, \quad w^* = w_0, \quad \text{at} \quad z^* = d,$$

where ω^* is the frequency of oscillations and ε is a very small positive constant.

The integration of the continuity eq. (1) under boundary conditions (4) for w^* gives, $w^* = w_0$. Substituting $w^* = w_0$ and eliminating the modified pressure gradient, under the usual boundary layer approximations, *i.e.* from eq. (2), we get,

$$U_t^* + \sigma B_0^2 U^*/\rho = -p_x^*/\rho.$$

Also from eq. (3), we obtain

$$2\Omega^* U^* = -p_y^*/\rho$$

Substituting the above pressure gradients in eqs. (2) and (3), we get

$$u_t^* + w_0 u_z^* = \upsilon u_{zz}^* + U_t^* + 2\Omega^* \nu^* \quad \frac{\sigma B_0^2}{\rho}\left(u^* - U^*\right), \tag{5}$$

$$\nu_t^* + w_0 \nu_z^* = \upsilon \nu_{zz}^* \quad 2\Omega^* \left(u^* - U^*\right) \quad \frac{\sigma B_0^2 \nu^*}{\rho}. \tag{6}$$

Introducing the following non-dimensional quantities

$\eta \quad z^*/d, \quad t - \omega^* t^*, \quad u = u^*/U_0, \quad \nu = \nu^*/U_0, \quad \Omega = \Omega^* d^2/\upsilon$ the rotation parameter,

$\omega - \omega^* d^2/\upsilon$ the frequency parameter, $s = w_0 d/\upsilon$ the injection/suction parameter and

$M - B_0 d\sqrt{\frac{\sigma}{\mu}}$ the Hartmann number, we get,

$$\omega u_1 + s u_\eta = u_{\eta\eta} + \omega U_t + 2\Omega\nu - M^2(u - U), \tag{7}$$

$$\omega \nu_t + s\nu_\eta = \nu_{\eta\eta} - 2\Omega(u - U) - M^2\nu. \tag{8}$$

The corresponding tranformed boundary conditions become

$$\left.\begin{aligned} &u = \nu = 0 && \text{at } \eta = 0, \\ &u = U(t) = 1 + \varepsilon \cos t, \quad \nu = 0 \text{ at } \eta = 1. \end{aligned}\right\} \tag{9}$$

Eqs. (7) and (8) can now be combined into a single equation, by introducing a complex function $q = u + i\nu$, as

$$\omega q_t + s q_\eta = q_{\eta\eta} + \omega U_1 - 2i\Omega(q - U) - M^2(q - U), \tag{10}$$

and the boundary conditions (9) can also be written in complex notations as

$$\begin{aligned} &q = 0 && \text{at} \quad \eta = 0, \\ &q = (U)(t) = 1 + \frac{\varepsilon}{2}\left(e^{it} + e^{-it}\right) \text{at} \quad \eta = 1. \end{aligned} \tag{11}$$

In order to solve eq. (10) subject to the boundary conditions (11), we look for a solution of the form

$$q(\eta, t) = q_0(\eta) + \frac{\varepsilon}{2}\left\{q_1(\eta)\, e^{it} + q_2(\eta)\, e^{-it}\right\} \tag{12}$$

substituting (12) into (10) and (11) comparing the harmonic and nonharmonic terms, we get

$$q_0'' - sq_0' - \left(l^2 + M^2\right) q_0 = -\left(l^2 + M^2\right), \tag{13}$$

$$q_1'' - sq_1' - \left(m^2 + M^2\right) q_1 = -\left(m^2 + M^2\right), \tag{14}$$

$$q_2'' - sq_2' - \left(n^2 + M^2\right) q_2 = -\left(n^2 + M^2\right), \tag{15}$$

where $l^2 = i2\Omega$, $m^2 = i(2\Omega + \omega)$ and $n^2 = i(2\Omega - \omega)$.

The corresponding transformed boundary conditions

$$\begin{aligned} &q_0 = q_1 = q_2 = 0 \quad at \quad \eta = 0, \\ &q_0 = q_1 = q_2 = 1 \quad at \quad \eta = 1. \end{aligned} \tag{16}$$

The solutions of eqs. (13) to (15) under the boundary conditions (16) are obtained as

$$q_0(\eta) = 1 - \left(e^{(r_1 + r_2\eta)} - e^{(r_2 + r_1\eta)}\right) \Big/ \left(e^{r_1} - e^{r_2}\right), \tag{17}$$

$$q_1(\eta) = 1 - \left(e^{(r_3 + r_4\eta)} - e^{(r_4 + r_3\eta)}\right) \Big/ \left(e^{r_3} - e^{r_4}\right), \tag{18}$$

$$q_2(\eta) = 1 - \left(e^{(r_5 + r_6\eta)} - e^{(r_6 + r_5\eta)}\right) \Big/ \left(e^{r_5} - e^{r_6}\right), \tag{19}$$

where

$$r_1 = \left(s + \sqrt{s^2 + 4\left(l^2 + M^2\right)}\right) \Big/ 2, \quad r_2 = \left(s - \sqrt{s^2 + 4\left(l^2 + M^2\right)}\right) \Big/ 2,$$

$$r_3 = \left(s + \sqrt{s^2 + 4\left(m^2 + M^2\right)}\right) \Big/ 2, \quad r_4 = \left(s - \sqrt{s^2 + 4\left(m^2 + M^2\right)}\right) \Big/ 2,$$

$$r_5 = \left(s + \sqrt{s^2 + 4\left(n^2 + M^2\right)}\right) \Big/ 2, \quad r_6 = \left(s - \sqrt{s^2 + 4\left(n^2 + M^2\right)}\right) \Big/ 2.$$

3. Results and discussion

Now for the resultant velocities and the shear stresses of the steady and unsteady flow, we write

$$u_0(\eta) - i\nu_0(\eta) = q_0(\eta) \tag{20}$$

and

$$u_1(\eta) - i\nu_1(\eta) = q_1(\eta)\, e^{it} + q_2(\eta)\, e^{-it}. \tag{21}$$

The solution (17) corresponds to the steady part which gives u_0 as the primary and ν_0 as the secondary velocities for the steady flow are given by

$$R_0 = \sqrt{u_0^2 + \nu_0^2}, \quad \theta_0 = \tan^{-1}(\nu_0/u_0). \tag{22}$$

In Figure 1a, the resultant velocity R_0 is shown graphically for samll and large values of rotations when the suction velocity and the magnetic field strenght vary. This figure shows that for small rotation Ω (curves I, II) and increase in the injection/suction parameter s leads to a decrease in the resultant velocity R_0 everywhere in the

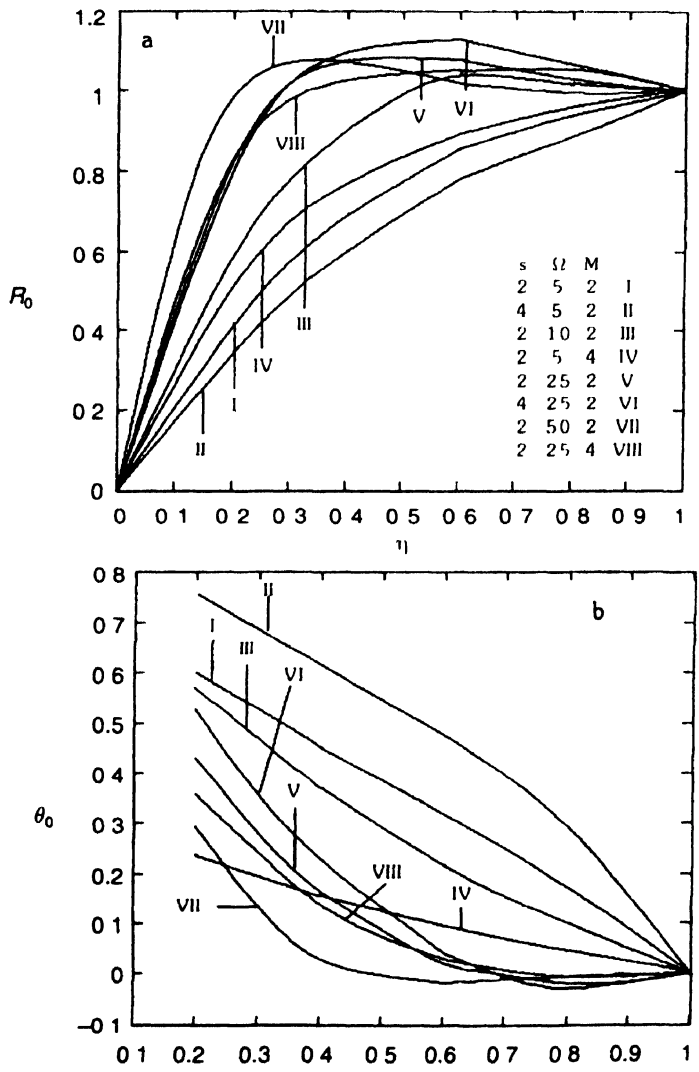

Figure 1(a & b). Resultant velocity R_0 and phase angle θ_0 due to u_0 and ν_0.

channel, however, the resultant velocity R_0 decreases near the stationary plate but increases near the oscillating plate, when rotation is large (curves V, VI) An increase in the small values of rotation Ω, an increase in R_0 is observed in the whole width of the channel (curves I, III), whereas increase in large rotation reveals that in the lower half of the channel resultant velocity R_0 increases but then it decreases in the upper half of the channel (curves V, VII) The increase in the magnetic field strength represented by the Hartmann number M leads to an increase in R_0 everywhere in the channel for small rotations (curves I, IV), but for large rotations there is a slight increase near the stationary plate, but a significant decrease in R_0 thereafter (curves V, VIII) For large rotations R_0 rises within a very short distance from the stationary plate to the value unity and oscillate about it

Figure 1b, shows that for small rotations Ω the phase angle θ_0 for the steady flow increases with the injection/suction parameter s but decreases with the increase of rotation parameter Ω and the Hartmann number M in the whole width of the channel (curves I, II, III, IV) For large rotations the increase in injection/suction parameter s gives rise to an increase in the phase lead everywhere in the channel except a slight decrease in the phase lag near the oscillating plates (curves V VI) Also the increase in rotation Ω (curves V, VII) leads to a decrease in phase lead and phase lag in the lower half of the channel and upper half of the channel respectively A phase lag is also evident from this figure near the upper oscillating plate for large rotations The increase in the magnetic field strength represented by the Hartmann number M leads to a decrease in θ_0 for large rotations near the stationary plate but a slight increase in θ_0 thereafter (curves V, VIII)

The amplitude and the phase difference of shear stresses at the stationary plate ($\eta = 0$) for the steady flow can be obtained as,

$$\tau_{0r} = \sqrt{\tau_{0x}^2 + \tau_{0y}^2}, \quad \theta_{0r} - \tan^{-1}\left(\tau_{0y}/\tau_{0x}\right) \tag{23}$$

where

$$\tau_{0x} + i\tau_{0y} - \left(\partial q/\partial \eta\right)_{\eta\ 0} = \left(r_1 e^{r_2} - r_2 e^{r_1}\right)\Big/\left(e^{r_1} - e^{r_2}\right) \tag{24}$$

Here τ_{0x} and τ_{0y} are, respectively, the shear stresses at the stationary plate due to the primary and secondary velocity components. The numerical values of the amplitude τ_{0r} of the steady shear stress and the phase difference of the shear stresses at the stationary plate ($\eta = 0$) for the steady flow are presented in Table 1 This table clearly shows that τ_{0r} increases with the increase of Ω for all values of rotation large or small It is also evident from the values in this table that τ_{0r} decreases with increase of injection/suction parameter s Also the increase in the magnetic field strength represented by Hartmann number M leads to an increase of τ_{0r} for all values Ω large or small, however, the increase is insignificant for large values of rotations The phase difference θ_{0r} increases with the increase of Ω for small rotations but decreases with

Table 1. Values of τ_{0r} and θ_{0r} for various s Ω and M

s	Ω	M	τ_{0r}	θ_{0r}
2	5	2	2 52905	0 7663
4	5	2	1 9657	0 9042
2	10	2	3 80846	0 82642
2	5	4	3 48486	0 34098
2	25	2	6 38222	0 8409
4	25	2	5 74232	0 93402
2	50	2	9 30726	0 83454
2	25	4	6 48027	0 71149

for large rotations. With the increase of injection/suction parameter s, θ_{0r} increases for both small and large rotations. Also the increase of Hartmann number leads to a decrease of θ_{0r} for any values of rotation small or large

The solutions (18) and (19) together give the unsteady part of the flow The unsteady primary and secondary velocity components $u_1(\eta)$ and $v_1(\eta)$, respectively, for the fluctuating flow can be obtained as

$$u_1(\eta, t) = \{\text{Real} q_1(\eta) + \text{Real} q_2(\eta)\} \cos t - \{\text{Im}\, q_1(\eta) - \text{Im}\, q_2(\eta)\} \sin t, \tag{25}$$

$$v_1(\eta, t) = \{\text{Real} q_1(\eta) - \text{Real} q_2(\eta)\} \sin t + \{\text{Im}\, q_1(\eta) + \text{Im}\, q_2(\eta)\} \cos t, \tag{26}$$

The resultant velocity or amplitude and the phase difference of the unsteady flow are given by

$$R_1 = \sqrt{u_1^2 + v_1^2}, \quad \theta_1 = \tan^{-1}(v_1/u_1) \tag{27}$$

For the unsteady part, the resultant velocity or the amplitude, R_1 and the phase angle, are presented graphically in Figure 2a,b for the two cases of rotation, Ω small (5 10) and Ω large (25,50) Figure 2a shows that with increase of injection/suction parameter s the resultant velocity R_1 decreases (curves I, II) for small rotations but increases (curves VI, VII) for large rotations except in the vicinity of the stationary plate For small values of Ω the amplitude R_1 increases (curves I, III) with increase of rotation, however, for large values of rotation Ω, the amplitude R_1 increases (curves VI, VIII) in the lower half of the channel and decreases in the upper half The resultant velocity R_1 increases with increase of Hartmann number M for small rotations (curves I, IV) but decreases with M for large rotations throughout the width of the channel (curves VI, IX). Keeping all the parameters s, Ω and M fixed, an increase in the frequency of oscillations ω leads to a decrease of the resultant velocity R_1 (curves I, V) for small rotations but to a slight increase of R_1 (curves VI, X) for large values of rotations.

Figure 2b exhibits that the phase angle θ_1 increases (curves I, II) with the

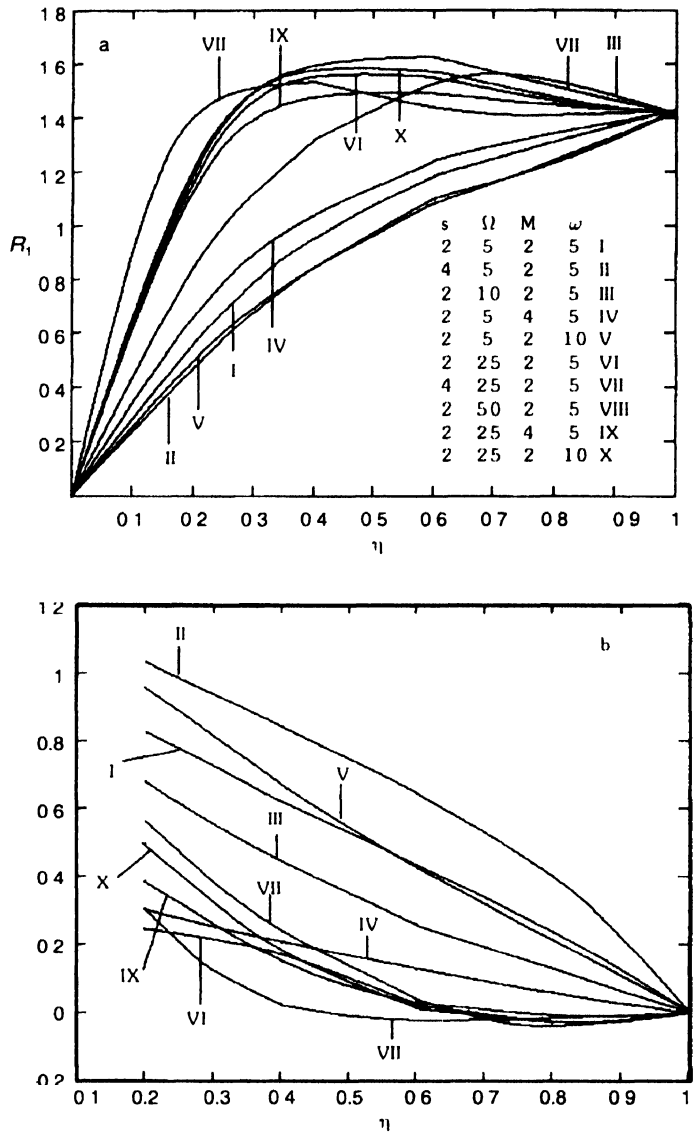

Figure 2(a & b). Resultant velocity R_1 and phase angle θ_1 due to u_1 and v_1.

increase of injection/suction parameter s in the whole width of the channel for small rotations; however, for large rotations although it increases in the lower part of the channel, it decreases in the upper part (curves VI, VII). In both the cases of small or large rotations θ_1 decreases with the increase of Ω (curves I, III and VI, VIII). For small rotations θ_1 decreases with the increase of Hartmann number M (curves I, IV) but for large rotations it oscillates (curves VI, IX). The increase of frequency of oscillations ω leads to an increase in the lower half of the channel and a decrease in the upper half of the channel for small rotations (curves I, V) but for large rotations the phase angle θ_1 oscillates (curves VI, X). It is also noticed that with the increase

of frequency of oscillations ω the phase lead turns into phase lag near the upper oscillating plate where it becomes approximately zero.

For the unsteady part of the flow, the amplitude and the phase difference of shear stresses at the stationary plate ($\eta = 0$) can be obtained as

$$\tau_{1x} + i\tau_{1y} = (\partial u_1/\partial\eta)_{\eta=0} + i(\partial v_1/\partial\eta)_{\eta=0} \tag{28}$$

which gives

$$\tau_{1r} = \sqrt{\tau_{1x}^2 + \tau_{1y}^2}, \quad \theta_{1r} = \tan^{-1}(\tau_{1y}/\tau_{1x}) \tag{29}$$

The amplitude τ_{1r} of the unsteady shear stress is shown graphically in Figure 3. The figure clearly shows that the amplitude τ_{1r} increases for both small and large values

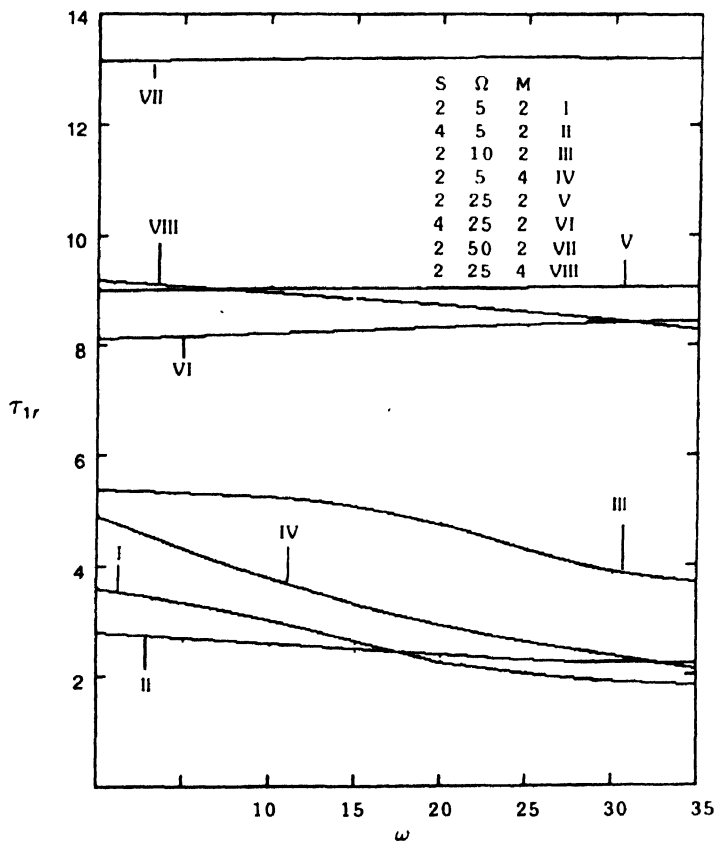

Figure 3. The amplitude τ_{1r} of unsteady shear stress for $t = \pi/4$.

of rotation parameter Ω (curves I, III and V, VII). For small values of Ω the figure also shows that τ_{1r} decreases with the increase of injection/suction parameter s and then increases for large values of frequency ω, however, τ_{1r} decreases with the increase of injection/suction parameter s for large rotations and for any value of frequency of oscillations ω (curves I, II and V, VI). The amplitude τ_{1r} increases with the Hartmann

number M for any value of the frequency and small rotations (curves I, IV), but for large rotations τ_{1r} decreases except for very small frequency (curves V, VIII). The numerical values of the phase difference θ_{1r} are listed in Table 2.

Table 2. Values of θ_{1r} for various s, Ω, M and ω.

s	Ω	M	ω							
			0	5	10	15	20	25	30	35
2	5	2	0 76221	1 0511	1.3258	1.52791	−1.4857	−1.39355	−1.32107	−1.25953
4	5	2	0.90106	1.2438	1.55176	1 54498	−1 16751	−1.03643	−0.93663	−0.85806
2	10	2	0.82669	0.9707	1.12026	1.28195	1.45032	−1.56719	−1.49379	−1.44407
2	5	4	0 34096	0.4345	0.5248	0.60515	0.6731	0.73041	0.78008	0.8247
2	25	2	0.84088	0.8960	0.95152	1.00771	1.6532	1.12523	1 18871	1.25773
4	25	2	0.9340	0.9947	1.05522	1.11601	1 17776	1.24129	1.30769	1.3784
2	50	2	0.83454	0.8613	0.88819	0.91511	0.94217	0.96946	0.99705	1.0250
2	25	4	0.71149	0 7631	0.81493	0.86727	0.9204	0.97459	1.03003	1.0866

It is interesting to note that there remains a phase lead with the increasing frequency of oscillations for large rotations; however, the phase lead changes to phase lag with increasing frequency of oscillations for small values of rotation Ω. In the case of small rotations, θ_{1r} increases for all values of frequency of oscillations with the increase of injection/suction parameter s. It is also evident from this table that with the increase of Hartmann number M, θ_{1r} decreases initially for small frequency of oscillations, but increases later on for large values of frequency of oscillations.

Acknowledgment

The authors are highly thankful to the referee for his valuable suggestions which led to a definite improvement of the paper.

References

[1] H A Attia and N A Kotb *Acta Mech.* **117** 215 (1996)

[2] J T Yen and C C Chang *Z. Angew. Math. Phys.* (ZAMP) **15** 400 (1964)

[3] C C Chang and T S Lundgren *Z. Angew. Math. Phys.* (ZAMP) **12** 100 (1961)

[4] V Vidyanidhu and S D Nigam *J. Math Phys. Sci.* **1** 85 (1967)

[5] A S Gupta *Acta Mech.* **13** 155 (1972)

[6] R N Jana and N Datta *Acta Mech.* **26** 301 (1977)

[7] A S Gupta *Phys. Fluids* **15** 930 (1972a)

[8] B S Mazumder *PhD Thesis* IIT Kharagpur (India)

[9] B S Mazumder, A S Gupta and N Datta *Int. J. Heat Mass Transfer* **19** 523 (1976)

[10] V M Soundalgekar and I Pop *J. Appl. Math. Mech.* (ZAMM) **53** 718 (1973)

[11] B S Mazumder *J. Appl. Mech.* **58** 1104 (1991)

[12] R Ganapathy *J. Appl. Mech.* **61** 208 (1994)

[13] K D Singh *J. Appl. Math Mech* (ZAMM) **80** 429 (2000)

[14] K D Singh, M G Gorla and Hans Raj *Indian J. Pure Appl. Math.* **36** 151 (2005)